

Carbon Paste Electrodes Obtained from Organic Waste After a Biodrying Process and Validation in an Electro-Fenton System Towards Alternative Valorization

A. Z. Vela-Carrillo¹, Luis A. Godínez², J. D. García-Espinoza², R. J. Martínez¹, M. O. Franco-Hernández³, A. B. Piña-Guzmán³, M. C. Santos⁴, F. Robles-Martínez^{3*}, I. Robles^{1*}

¹Centro de Investigación y Desarrollo Tecnológico en Electroquímica S. C., Parque Tecnológico Querétaro, 76703 Sanfandila, Pedro Escobedo, Querétaro, México.

²Facultad de Química, Universidad Autónoma de Querétaro, Cerro de Las Campanas SN, Querétaro, Querétaro 76010, México.

³Instituto Politécnico Nacional, Unidad Profesional Interdisciplinaria de Biotecnología, Av. Acueducto s/n, Barrio La Laguna, Col. Ticomán, CP 07340, México City, México.

⁴Laboratory of Electrochemistry and Nanostructured Materials (LEMN) – Center for Natural and Human Sciences (CCNH), Federal University of ABC (UFABC), CEP: 09210-170, Rua Santa Adélia 166, Bairro Bangu, Santo André, SP, Brazil.

*Corresponding author: F. Robles-Martínez, email: froblems@ipn.mx; I. Robles, email: irobles@cideteq.mx

Received February 1st, 2023; Accepted May 2nd, 2023.

DOI: <http://dx.doi.org/10.29356/jmcs.v67i4.1962>

Abstract. The transformation of agricultural waste into activated carbon represents an attractive approach as new and alternative source, but also as a reduction of pollution associated to the degradation of precursors.

The organic residues sugarcane (*Saccharum officinarum*) bagasse-shell, orange (*Citrus sinensis*) peel-bagasse, and eucalyptus (*Eucalyptus globulus*) leaves, obtained from a biodrying process were transformed into activated carbons using phosphoric acid as activating agent. The resulting materials were physicochemically characterized and after that, carbonaceous electrodes were prepared to test the feasibility of using them in a discoloration electro-Fenton wastewater treatment process. Orange peel-bagasse biodried precursor transformed into activated carbon showed the highest efficiency when used as the modifier in a carbon paste electrode due to its highest porosity, electroactive area ($24.9 \times 10^{-2} \text{ cm}^2$), and roughness (1.21 a.u.), also to its chemical affinity for anionic molecules. These properties, in addition to the capability of electro-sorb iron ions on the surface during the Fenton reaction, allowed a 44 % methyl orange discoloration efficiency. Sugarcane bagasse-peel and eucalyptus leaves biodried residues were also evaluated with efficiencies under 30 %, mainly attributed to intrinsic composition of the precursor materials.

Keywords: Activated carbon; agroindustrial waste; biodrying; carbon paste electrode; electro-Fenton; oxygen reduction reaction.

Resumen. La transformación de los residuos agrícolas en carbón activado representa un enfoque atractivo y novedoso, además de que representa una alternativa a la reducción de la contaminación asociada a la degradación de residuos orgánicos.

Los residuos orgánicos de bagazo de caña de azúcar (*Saccharum officinarum*), bagazo y cáscara de naranja (*Citrus sinensis*), y hojas de eucalipto (*Eucalyptus globulus*), que fueron obtenidos de un proceso de biosecado, se transformaron en carbón activado utilizando ácido fosfórico como agente activante. Los materiales resultantes se caracterizaron físicoquímicamente y después de eso, se prepararon electrodos de pasta de carbón modificados con estos materiales, para estudiar la viabilidad de utilizarlos en un proceso de tratamiento de aguas residuales

mediante electro-Fenton. El precursor biosecado de bagazo y cáscara de naranja transformado en carbón activado mostró la mayor eficiencia cuando se usó como modificador en un electrodo de pasta de carbón, debido a su mayor porosidad, área electroactiva ($24.9 \times 10^{-2} \text{ cm}^2$) y rugosidad (1.21), también debido a su mayor afinidad química por moléculas aniónicas. Estas propiedades, aunadas a la capacidad de electro-sorber iones de hierro en la superficie durante la reacción de Fenton, permitieron una eficiencia de decoloración del naranja de metilo del 44 %. También se evaluaron residuos biosecados de bagazo de caña de azúcar y hojas de eucalipto, con eficiencias inferiores al 30 %, atribuidas principalmente a la composición intrínseca de los materiales precursores.

Palabras clave: Carbón activado; residuos agroindustriales; biosecado; electrodos de pasta de carbón; electro-Fenton; reacción de reducción de oxígeno.

Introduction

Mexico stands out as a large producer of organic products, so there is a high production of agricultural and agroindustrial waste with a high composition of cellulose and hemicellulose that forms leachates [1,2] and biogas when those wastes are dumped. Therefore, residual biomass from both sectors, agricultural and agroindustrial, must be properly managed in order to avoid pollution problems. In this context, bio-drying is a process that allows to stabilize the residual biomass as a result of the dehydration of the materials (which in turn causes a low microbial activity) [3]. Thus, the application of bio-drying in the treatment of bio-waste contributes to the proper management of waste, facilitating its handling, transport, and storage. On the other hand, through bio-drying, biowaste is conditioned for the production of useful products leading to a sustainable circular bioeconomy.

In this regard, a useful approach of waste could be the production of activated carbon (AC) that can be used either for adsorption, or as cathode material for electrochemical advanced oxidation processes [4]. In addition, there are activated carbons of mineral and of organic origin and those obtained from the later source, have recently become particularly attractive due to the high availability of organic waste that can be used to prepare them.

Activated carbon features a wide variety of physical and chemical properties that makes it particularly suitable for the adsorption of a wide variety of contaminants [5,6]. The structural imperfections like porosity and morphology associated to a disorganized crystalline atomic structure, that characterize AC when compared to other carbonaceous materials such as graphite, are strongly related to the chemical activation process and the synthesis conditions [7,8].

In this way, the surface of AC is not only disordered when compared to other carbon materials, but also characterized by a relatively high electric conductivity (100 S/cm when treated above 1000° C) [7-11].

In this regard, activated carbon is not only a very good adsorbent substrate but also a good candidate for the development of cathode materials for electro-Fenton oxidation processes [12], in which the oxygen reduction reaction via two electrons ($2e^-$) in the presence of ferrous ions, gives rise to the strongly oxidant $\bullet\text{OH}$ (hydroxyl) radical species [9].

It is important to note that although there are several studies in the literature on the oxygen reduction reaction (ORR) in carbonaceous materials obtained from organic waste [13], to the best of our knowledge, few investigations focus on the use of agroindustrial-AC as mass modifiers for carbon paste electrodes to study the $2e^-$ oxygen reduction reaction, for example, Ortiz-Martinez *et al.* (2021) used orange peel and used coffee ground, Dhelipan *et al.* (2017) used orange peel, Chung (2017) used coffee ground, while Akula and Sahu (2019) and Srinu *et al.* (2018) employed used coffee grounds. All they reported the use of these activated carbons as mass-modifiers that favor the ORR due to the chemical and electrical properties of activated carbons that promote the electro-generation of H_2O_2 [14-18].

In this context, this study seeks to offer an alternative for the use of biodrying byproducts that consisted into the transformation of activated carbons by preparing modified carbon paste electrodes to carry out the oxygen reduction reaction so that these materials can find applications in electrochemical advanced oxidation processes. In this case, we used as a model molecule Methyl Orange in order to study its discoloration using an Electro-Fenton based system.

Experimental

Source and preparation of activated carbons

Three organic solid wastes (**sp**: sugarcane bagasse-shell; **ob**: orange peel-bagasse, and **eu**: eucalyptus leaves) were separately biodried in piles, in order to reduce weight and volume and to stabilize them biologically. Sugarcane bagasse-peel was collected from a Piloncillo Factory placed in Veracruz State, orange peel-bagasse was collected from a Juice Orange factory placed in Zacatenco community (México City) and eucalyptus leaves (foliage) were collected from a compost plant located in a university campus in north side of Mexico City.

The biodrying process lasted 45 days, the piles were turned once a week to favor gas exchange and aerate the material in order to promote microbial activity. In the present work, aeration was carried out by turning the piles manually with a shovel, which helps the loss of water (water vapor) and decreases the volumetric weight of the material in process, facilitating gas exchange after turning.

Once the materials were biodried, AC were prepared. For this purpose, the precursors (biodried materials as well as reference materials), were chemically activated for 24 h using phosphoric acid 0.6 M (from *Karal*) in a 2:1 mass ratio based on the report by Tovar *et al.* (2019), then were calcinated using a *Thermo Scientific Mini-mite* tubular oven, with a $150 \text{ cm}^3 \text{ min}^{-1}$ nitrogen atmosphere for the corresponding time and temperature [19]. Based on previous works, the precursor ob was carbonized at $600 \text{ }^\circ\text{C}$ [19], sp at $300 \text{ }^\circ\text{C}$ [20], and finally eu at $350 \text{ }^\circ\text{C}$, after testing some temperatures. After the carbonization process, activated carbons were washed with deionized water and dried in an *Felisa* oven at $85 \text{ }^\circ\text{C}$ for 24 hours. Finally, the samples were grounded in a porcelain mortar and then stored at room temperature until use.

Characterization of activated carbons

The surface morphologies of the samples were studied by means of Scanning Electron Microscopy (SEM) using a Jeol, *JSM-6510LV* instrument (15 keV). On the other hand, the elemental surface composition of the samples was obtained from Energy Dispersive X-ray Spectroscopy (EDS) using a Bruker instrument (with XFlash6110 detector). After that, functional groups of the AC surface were identified using Fourier Transform Infrared Spectroscopy (FTIR, *Perkin Elmer Spectrum GX*).

After that, Boehm titration was carried out to quantify acid and basic oxygenated functional groups according to the methodologies by Oickle and Fulazzaky [21, 22]. For this purpose, a sample of activated carbon was placed in contact with HCl, NaHCO_3 , Na_2CO_3 and NaOH 0.1 M for 24 h and 120 h, and then, the mass was separated from liquid and the resulting solutions were titrated with the corresponding solutions.

In addition, a potentiometric titration was done to assess the surface's basicity or acidity of the AC [23]. In this way, two samples of activated carbon were equilibrated with NaOH and HCl 0.5 M and titrated with HCl and NaOH, respectively. Finally, the pH at point of zero charge (PZC) was determined by titration using a 10 mg carbon sample that was equilibrated for 48 hours with 50 mL of water at different initial pH values (from 3 to 11). As reported by Adan-Mas (2021), the x-intercept of the graph of initial vs final pH corresponds to the PZC [24].

Finally, to validate the affinity to positive or negative surfaces, a sorption capacity test was carried out. For that it was necessary that activated carbons were homogenized and grinded to particle size smaller than $300 \text{ }\mu\text{m}$. Batch experiments were conducted using 25 mL glass bottles, the samples were maintained under constant temperature of $25 \pm 1 \text{ }^\circ\text{C}$ and stirring at 170 rpm using an incubator (Biobase BJPX-103B). Methyl orange (MO), from Hycel, 99% purity, and methylene blue (MB) from Sigma-Aldrich, 99 % purity, were selected as anionic and cationic model molecules, respectively, to study the sorption effect on the surface of activated carbons as well as their interactions between surface groups. All the experiments were done using 10 mL of model molecule solution at 1500 mg/L ([MO] = 4.6 mM; [MB] = 4.7 mM), and a constant activated carbon dose of 2 g/L.

Modified carbon paste electrode preparation

Modified carbon paste electrodes (MCPE) were prepared as reported by Ortiz-Martínez *et al.* (2021) by homogeneously mixing graphite (g), activated carbon from agroindustrial waste (sp, ob and eu), and silicone oil as the binder (B). Graphite and silicone oil were reagent grade obtained from Sigma-Aldrich [14].

Three types of MCPE were prepared with biodried modifiers, type 1: electrodes that contain sp, type 2: electrodes that contain ob, and type 3: electrodes that contain eu. In each case, the activated carbon was mixed with graphite (identified as the carbonaceous material mixture), and then a binder was added, in a final 70:30 (w:w) carbonaceous material:binder mass ratio. After homogenization, the paste was packaged in the bottom of a 10 mL syringe from which the needle was previously removed, and the electrical contact was established with a copper wire. The surface of each of the electrodes was renewed by expelling the edge of the electrode paste before each experiment.

Study of the electrochemical activity of MCPEs

A preliminary electrochemical assessment of each of the MCPEs was carried out by means of cyclic voltammetry experiments. For this purpose a BioLogic SP-50 potentiostat was used, the probe was done using 20 mL of 0.1 M HNO₃ (from *J.T. Baker*, 70 % purity) as supporting electrolyte, and 0.001 M [Fe(CN)₆]^{3-/4-} (from *Karal*, 99 % purity) as an electrochemically reversible probe molecule. While the MCPE was set up in the electrochemical cell as the working electrode, a platinum wire and Ag|AgCl were used as counter and reference electrodes, respectively. The electroactive area was calculated as reported by Ortiz-Martínez [14].

After that, the oxygen reduction reaction was studied by cyclic voltammetry, for this purpose the MCPE prepared with biodrying activated carbons were used as working electrodes, an Ag|AgCl as a reference, and a Pt wire as a counter electrode, respectively [25].

Hence, when the redox signal for oxygen reduction was identified for each MCPE, the reduction potential obtained from cyclic voltammetry was applied and hydrogen peroxide production was calculated after two hours. During these experiments, an oxygen-saturated Na₂SO₄ electrolyte was employed [0.05M, *Baker*, 99 % purity]. To quantify the amount of electro-generated hydrogen peroxide (H₂O₂), titanium (IV) sulphate (from *J.T. Baker*, 99 %) was used as an indicator [26], and finally, the quantification was carried out by spectrophotometric measurements at 408 nm with a UV/Vis spectrophotometer (*Genesys 10S, Thermo Scientific*).

Evaluation of the performance of the CPE using electro-Fenton experiments

Finally, to evaluate the performance of the carbon paste electrodes, the discolouration of methyl orange to test the feasibility of the electrodes as new materials in the Fenton processes. In these regards, electro-Fenton experiments were carried out in 15 mL of a Na₂SO₄ [0.05 M] electrolytic cell, the pH was adjusted to pH 3, a 20 mg L⁻¹ of methyl orange concentration and 0.3 mg L⁻¹ of dissolved iron (FeSO₄, from *JT Baker*, 99%) were added to the electrolytic oxygen saturated solution. Then, the corresponding oxygen reduction potential was imposed for two hours, and the colour removal was followed using UV-Vis spectroscopy. A reference was also followed in the absence of oxygen and iron cations.

Results and discussion

Physicochemical characterization of carbonaceous materials

Fig. 1 (a-d) shows SEM micrographs of the activated carbons obtained from organic bioprocessed waste compared to graphite. The activated carbon samples are characterized by a disordered and porous structure, as it can be seen for the three kinds of AC in Fig. 1(a), 1(b), and 1(c), which is different when compared to graphite (see Fig. 1(d)). The porous structure belongs to the composition of the precursor, and this can be related to the roughness and the performance of each material discussed later in section 3.4. From the literature, it is known that the most porous material corresponds to the substrate with the larger content of lignin and cellulose [27].

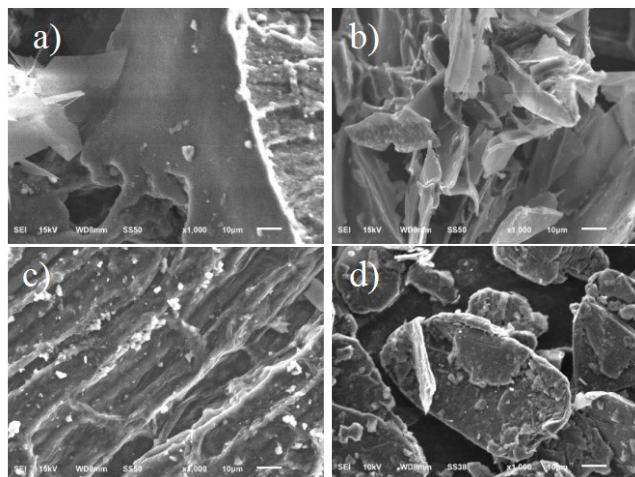


Fig. 1. Scanning electron micrographs of activated carbons obtained from: **(a)** sugarcane bagasse-peel (sp); **(b)** orange peel-bagasse (ob); **(c)** eucalyptus leaves (eu); **(d)** graphite (g) as reference. Magnification of 1000x.

The results of the elemental composition obtained from EDS, potentiometric titration, Boehm titration, point of zero charge (PZC), and sorption capacity are shown in Table 1, corresponding to three activated carbons (sp, ob and eu), as well as reference materials (sb, op, and g). It is possible to point out that the reference materials were: orange peel without bagasse (op), and sugarcane bagasse without peel (sb). Graphite (g) was also included since this material was used to improve the electric conductivity in the CPE, as it will be later discussed in the modified electrodes section.

These results are arranged from the lowest to the highest PZC value from biodried source materials, which can be directly correlated to pKa value of their surface. From inspection of Table 1, it is possible to appreciate that biodried materials have a predominant affinity to anions as verified by sorption capacity data that showed a higher sorption capacity for methyl orange than for methylene blue, that give evidence of the affinity to anions by the -predominantly- positive surface of all the samples.

The C/O ratio showed a value around 2 for most of the materials, however, eu showed a higher value compared to organic activated carbons.

From the FTIR data in Fig. 2, it is possible to identify vibrations corresponding to esters, lactones and quinones, given by signals between 2310 and 2385 cm^{-1} , and carboxylic acid, phenol, and ester groups around 1380 cm^{-1} , those groups correspond to C-O-H_(s) and C-O-R_(s) bonds.

On the other hand, the band around 1550–1680, or 1660–1670 cm^{-1} , are generally assigned to quinone groups, but also the band at 1660 cm^{-1} is assigned either to aromatic C=C stretching vibration of the basal planes and oxygen surface compounds [29]. It is well known that all these compounds are derivate products of lignocellulose, cellulose, and lignin [30,31].

The presence of oxygenated functional groups around 2310 and 1380 cm^{-1} facilitates the ORR, due to the surface groups containing oxygen are considered the most important due to the strong propensity of the planes in the structure of the AC to chemisorb oxygen [11,32,33]. The reason is mainly attributed to the chemisorbed molecular oxygen that is dissociated into atoms that can chemically react with carbon atoms to form surface oxygenated compounds. Oxygen functional groups are active sites that promote the two-electron oxygen reduction reaction [34].

Additional to that signals, is possible to see non-oxygenated groups in both materials, that could be associated to aliphatic groups (C-H) at 596 cm^{-1} , esters of acid phosphate (P-O) at 1070 cm^{-1} , alkene and carboxylate (C=C_(s)) at 1626 cm^{-1} , and hydroxyl and polysaccharide (-OH_(s)) at 3422 cm^{-1} [35,36].

Finally, the signal of P-O vibration is also attributed to the remaining phosphorous from the activation stage during the AC preparation [14].

It is important to point out that the presence of oxygenated groups favours the oxygen reduction reaction but also, the oxygenated acid species provides good electroactivity towards hydrogen peroxide electro-generation, that is related to the high hydrophilicity, high conductivity, and due to the sorption of the O₂ molecule on carbon modified surfaces, by Pauling model [11,32,37].

Table 1. Results obtained from chemical characterization by EDS (Energy Dispersive X-ray Spectroscopy), potentiometric titration, Boehm titration, pH of point of zero charge, and sorption capacity.

Parameter		Obtained from biodrying process			Reference materials [28]		
		sp	ob	eu	sb	op	g
Elemental composition, EDS (%)		C=62.99, O=31.77, P= 4.86, S= 0, Others= 0.38	C=43.91, O=23.86, P= 22.75, S= 0, Others= 9.48	C=81.52, O=16.89, P= 1.11, S= 0, Others= 0.48	C=68.72; O=24.41; P=6; S=0 Others= 0.87	C=33.88 O=34.30 P= 18.18 S= 0 Others= 13.64	C=96.3, O=2.99, P= 0, S= 0, Others= 27.44
C/O, EDS (a.u.)		1.98	1.84	4.83	2.82	0.99	32.21
Boehm titration	Acid groups (meq/g)	2.08 ± 0.085	1.74 ± 0.117	1.73 ± 0.257	2.51 ± 0.257	1.3 ± 0.117	1.08 ± 0.169
	Basic groups (meq/g)	0.21 ± 0.108	0.68 ± 0.061	0.01 ± 0.240	1.33 ± 0.240	1.1 ± 0.061	1.20 ± 0.071
Predominant affinity given by potentiometric titration		Positive surface, anion affinity	Positive surface, anion affinity	Positive surface, anion affinity	Positive surface, anion affinity	Positive surface, anion affinity	Negative surface, cation affinity
PZC (a.u.)		2.10 ± 0.007	2.51 ± 0.007	3.02 ± 0.035	2.05 ± 0.035	2.05 ± 0.007	7.22 ± 0.368
Sorption capacity	MO (mg/g)	137.53 ± 1.68	292.03 ± 14.72	189.05 ± 5.69	44.93 ± 9.973	104.129 ± 15.08	0.00 ± 0.00
	MB (mg/g)	112.95 ± 33.18	53.94 ± 10.36	16.71 ± 0.77	117.55 ± 9.660	74.150 ± 6.251	12.15 ± 0.64

PZC: point of zero charge; MO: methyl orange; MB: methylene blue

Biodried materials are: sp (sugarcane bagasse-peel), ob (orange peel with bagasse), eu (eucaliptus), and reference materials are: sb (shelled cane bagasse), op (orange peel without bagasse), and g (graphite).

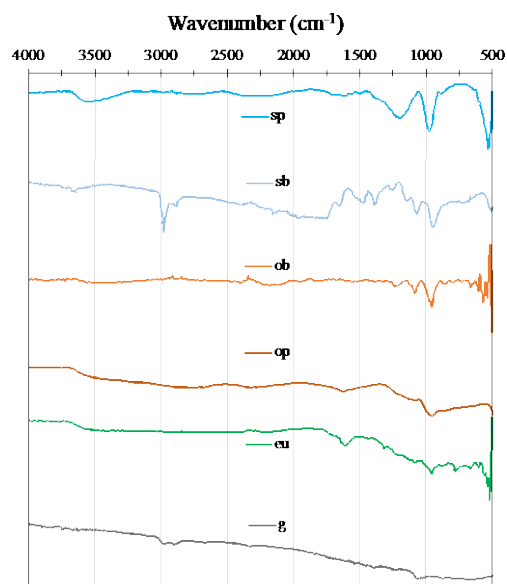


Fig. 2. FTIR spectra comparison of AC obtained from biodrying process: sugarcane bagasse-shell (sp), orange peel with bagasse(ob), eucalyptus leaves (eu); and reference materials: graphite (g), orange peel without bagasse (op), shelled cane bagasse (sb).

Electrochemical performance of MCPE

Some of the most important parameters for MCPEs are mechanical stability and conductivity [38], to promote a good performance, these conditions were achieved using a 70:30 (w:w) carbonaceous material:binder mass ratio as reported by Ortiz-Martínez, where the carbonaceous material consists on the mixture of graphite and activated carbon [14]. The particle size of graphite ranges from 180 to less than 75 μm , the size of the activated carbon particles range from 250 to less than 75 μm , and therefore, it can be assumed that samples with a higher proportion of small graphite particles (diameter smaller than 75 μm), will be better packed since empty sites between AC particles can be occupied with graphite units, and this should facilitate the electric conductivity of the composite material as well as the performance of the MCPE.

Fig. 3 shows the cyclic voltammograms of **a)** g, **b)** sp, **c)** ob, and **d)** eu. From the corresponding voltammograms, the ΔE (E) as well as the cathodic (E_c) and anodic peak (E_a) potentials can be identified from inspection of blue zone (see Fig. 3), and from these signals it is possible to infer that as expected, the modified electrodes show a quasi-reversible behavior [39,40].

Electroactive areas and roughness factors were calculated from cyclic voltammogram responses in Fig. 3 as reported by Ortiz-Martínez [14]. The determination of a surface roughness factor refers to the ratio obtained from the real area/geometric area, referred to the real surface of the active sites. The results of these calculations are shown in Table 2. From the corresponding data, it can be readily seen that ob has the highest electroactive area and roughness, compared to eu and sp, even when compared to the corresponding material op, for this reason it is assumed that the bagasse in ob modify the C/O ratio as well as the acid groups determined by Boehm titration, and these properties may promote the higher electroactive area and roughness values.

From the electrochemical response data using a reversible ferro/ferri probe molecule (Fig. 3), it is possible to see that MCPEs modified with activated carbons obtained from agroindustrial source constitute an attractive alternative to study electrochemical processes such as the 2e⁻ oxygen reduction reaction since these carbonaceous materials are not only particularly stable but also of abundance and low cost [34].

In this context, elemental analysis of the activated carbons (see Table 1), revealed that the composite is mostly characterized by carbon and oxygen content, and as reported by Švancara *et al.* (1996) a high content of oxygen in carbon electrodes favors the 2e⁻ cathodic reduction of molecular oxygen beneficial for the oxygen reduction reaction [41].

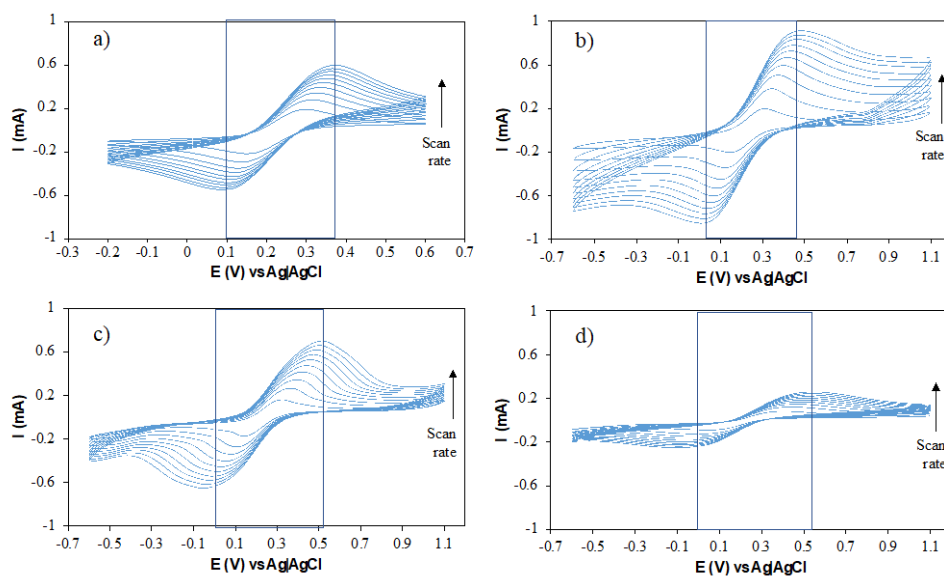


Fig. 3. Cyclic voltammograms of (a) g, (b) sp, (c) ob, (d) eu; $[\text{Fe}(\text{CN})_6]^{3-/4-}$ [0.001M], pH 3. Reference electrode: Ag|AgCl, Counter Electrode: Platinum wire, scan rate ranged from 10-100 mV/s.

Study of oxygen reduction reaction

The potential of oxygen reduction was identified for sp, ob, and eu, and bare graphite by means of cyclic voltammetry experiments in oxygen and nitrogen saturated, Na_2SO_4 [0.05M] solutions. The responses obtained from the experiments carried out under pH 3 are shown in Fig. 4. Inspection of the corresponding data shows that the oxygen reduction signal appears at around -0.5 V to -0.9 V vs Ag|AgCl, but specifically for sp it was not possible to identify the reduction signal although the different scan rate evaluation.

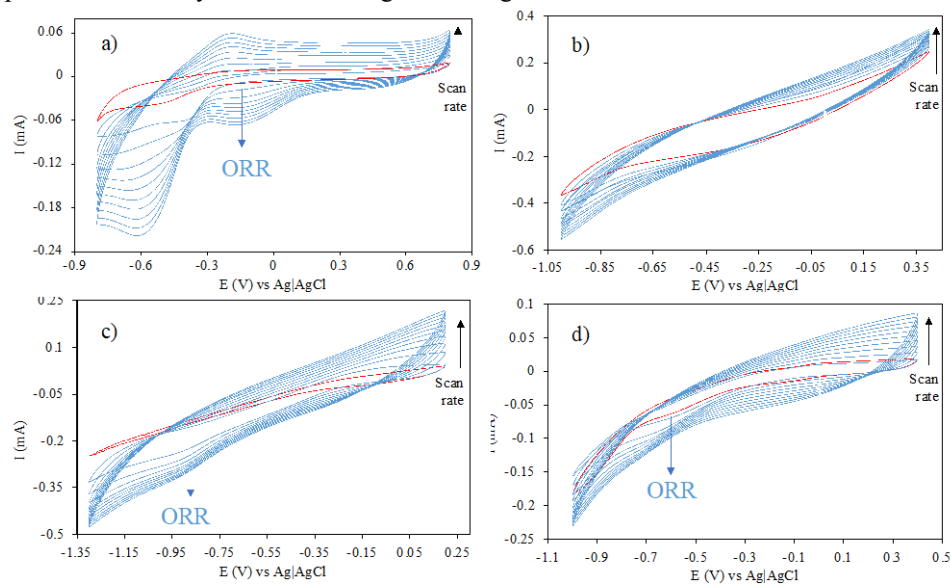


Fig. 4. Cyclic voltammograms of oxygen reduction reaction on the surface of (a) GPE, (b) sp, (c) ob, (d) eu; red line represents absence of O_2 , Reference electrode: Ag|AgCl, Counter electrode: Platinum wire; pH 3 in Na_2SO_4 [0.05M], scan rate ranged from 10-100 mV/s.

In order to confirm the 2e- oxygen reduction reaction on the different substrates under study, the electrochemical generation of hydrogen peroxide was evaluated. In this way, a reduction potential of -0.7 V vs Ag|AgCl (for electrodes modified with sp, ob and eu), was imposed and the amount of hydrogen peroxide was determined. After two hour-experiments, the amount of hydrogen peroxide ranged between 0.5-1 mg L⁻¹ for all electrodes, similar values were reported by Ortiz-Martínez [14]. These results confirm the possibility to use activated carbons as modifiers in carbon paste electrodes.

Polarized carbonaceous materials are usually employed as cathode materials to produce hydrogen peroxide *in situ* by means of the two-electron oxygen reduction reaction, the structural organization of carbon atoms and oxygen-containing groups facilitate the electron transfer, and the hydrogen peroxide could easily be produced [14,42,43].

Electro-Fenton validation experiments

Electro-Fenton experiments using the different carbon paste electrodes under study were performed in order to assess the potential of these materials for the development of advanced oxidation processes. After two-hour experiments, the color removal for each system was as follows: ob > sp > eu, see Table 2 and Fig. 5. These results show the feasibility of paste electrodes modified with activated carbons of a biodrying source, to be implemented in electrochemical advanced oxidation processes. From inspection of table 2 is possible to assume that the highest discoloration efficiency the highest electroactive area as well as the roughness, directly related to the morphology previously discussed in section 3.1, where ob seem to be the most porous material compared to sp and eu. Another important contribution from ob is its chemical composition since this material showed the highest methyl orange sorption capacity, that indicates the highest surface affinity.

From inspection of Fig. 4, it was pre-assumed that the reduction of oxygen could not be possible on the surface of MCPE modified with ob, because no reduction signal was identified. Similar findings were reported by Ortiz-Martínez, they reported a similar behavior for a MCPE modified with spent coffee ground activated carbon, where no reduction signal appear in the voltametric study, but this was the most efficient material when evaluated for discoloration, with 99 % efficiency in 2 hours. It was assumed that the Fenton efficiency can be attributed to higher capacitive current, since the Fenton process is directly proportional to the adsorption of iron cations on the surface and inversely proportional to the faradaic current of the oxygen reduction reaction, which in turn is related to oxygenated groups in the surface of the material [14,44].

On the other hand, it is well known that a wide variety of carbonaceous materials are capable to produce H₂O₂, many reports in the literature refer to the electro-Fenton decomposition of model dye pollutants. However, few carbonaceous materials from organic source have been studied for that purpose. In this regard, Ortiz-Martínez *et al.* (2021) reported the use of orange peel, without bagasse, in a similar process, and the reported efficiency was 59 % (see Table 2) [14]. The differences could be associated to the source of the material that may influence the feasibility of the Fenton reaction.

Table 2. Comparison of carbon paste electrodes.

Parameter	Obtained from biodrying process			Reference materials [14]	
	sp	ob	eu	g (bare electrode)	op
Electroactive area (cm ²)	5.7x10 ⁻²	24.9x10 ⁻²	15.05x10 ⁻²	3.52x10 ⁻⁴	1.18x10 ⁻²
Roughness (a.u.)	0.28	1.21	0.74	1.72x10 ⁻³	5.77x10 ⁻²
Blank discoloration in absence of iron and oxygen, (%)	7.50	9.86	9.01	*ND	*ND
Electro-Fenton efficiency (%)	31.68	47.76	24.32	54.54	59.09

*ND- not determined

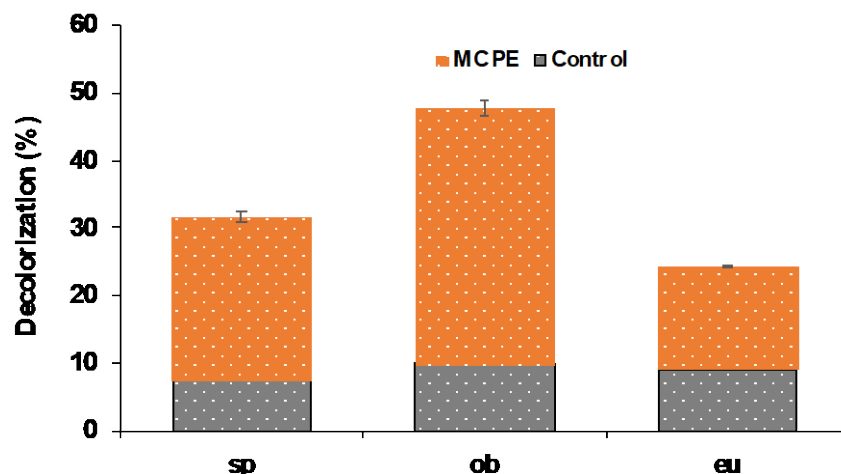


Fig. 5. Discoloration efficiency comparison for modified carbon paste electrodes.

It can be assumed from the inspection of the data in Table 2 and reference materials that the presented higher discoloration efficiency than those electrodes containing AC from biodried materials (sp, ob, and eu), however since the electrochemical response resulted in high electroactive areas, those electrodes might be used to study other electrochemical reactions with lower capacitive requirements.

The different current response in electrodes is associated with capacitive current which depends on physical and chemical composition of the precursor material [45,46]. Oxygenated functional groups influence the electrochemical properties of carbon materials, in this regard, the capacitance provided by hydroxyl and quinone groups is higher than that provided by carboxyl groups in acidic-aqueous electrolytes. All these groups are clearly defined in all the studied activated carbons (see Fig. 2) [14,46].

Conclusions

This study shows the feasibility of use organic materials obtained after a biodrying process. In this way, activated carbons from biodried organic waste were prepared and evaluated as a source of composite materials in modified carbon paste electrodes, resulting in substrates that constitute a good alternative for using them in electrochemical experiments.

The electrochemical experiments showed that these materials are not only a good alternative for the study of oxygen reduction reactions, but also the electrochemical performance show a good capability to study other heterogeneous electron transfer processes.

Activated carbon obtained from the biodrying of orange peel-bagasse resulted to be the most adequate material since it exhibits a porosity structure that promotes the highest electroactive area and roughness; these properties were developed from the thermochemical activation method as well from the precursor, and those are directly related to the anion affinity to methyl orange among others. Although this material did not show a well-defined electro-reduction signal, the highest Fenton efficiency may be attributed to the coupled process of iron cations retention on the surface of the electrode that improves the development of the Fenton reaction.

This study shows promising results also to study other electrochemical reactions since the responses are stable and comparable to reports from the literature. This study showed that the proposed approach is a good choice to explore new alternatives to take advantage of biodried materials.

Acknowledgements

The authors express their gratitude to the Mexican Council for Science and Technology, (CONACYT: CB-2019-01-285309, and PENTA 2019-1-303758), and Secretaría de Investigación y Posgrado from Instituto Politécnico Nacional (Mexico), for the financial support of this work. Authors also thank to CIDETEQ and UFABC collaborative research agreement and FAPESP Brazil (2017/10118-0). The authors are also grateful to Fabricio Espejel for SEM analysis. A. Vela-Carrillo also thanks CONACYT for her graduate fellowship.

References

1. Mata, T. M.; Martins, A. A.; Caetano, N. S. *Bioresour. Technol.* **2018**, *247*, 1077–1084. DOI: <https://doi.org/10.1016/j.biortech.2017.09.106>.
2. Ballesteros, L. F.; Teixeira, J. A.; Mussatto, S. I. *Food Bioproc. Tech.* **2014**, *7*, 3493–3503. DOI: <https://doi.org/10.1007/s11947-014-1349-z>.
3. Colomer-Mendoza, F. J.; Robles-Martinez, F.; Herrera-Prats, L. *Environ. Dev. Sustain.* **2012**, *14*, 1013–1026. DOI: <https://doi.org/10.1007/s10668-012-9369-1>.
4. Gonçalves, M.; Guerreiro, M. C.; Ramos, P. H. *Water Sci. Technol.* **2013**, *68*, 1085–1090. DOI: <https://doi.org/10.2166/wst.2013.349>.
5. Sahu, J. N.; Acharya, J.; Meikap, B. C. *Bioresour. Technol.* **2010**, *101*, 1974–1982. DOI: <https://doi.org/10.1016/j.biortech.2009.10.031>.
6. Yang, J.; Qiu, K. J. *Chem. Eng.* **2011**, *167*, 148–154. DOI: <https://doi.org/10.1016/j.ccej.2010.12.013>.
7. Biscoe, J.; Warren, B. E. *J. Appl. Phys.* **1942**, *13*, 364–371. DOI: <https://doi.org/10.1063/1.1714879>.
8. Lillo-Ródenas, M. A.; Carratalá-Abril, J.; Cazorla-Amorós, D.; Linares-Solano, A. *Fuel Process. Technol.* **2002**, *77–78*, 331–336. DOI: [https://doi.org/10.1016/S0378-3820\(02\)00073-5](https://doi.org/10.1016/S0378-3820(02)00073-5).
9. Figueiredo, J. L.; Pereira, M. F. R.; Freitas, M. M. A.; Órfão, J. J. M. *Carbon.* **1999**, *37*, 1379–1389. DOI: [https://doi.org/10.1016/S0008-6223\(98\)00333-9](https://doi.org/10.1016/S0008-6223(98)00333-9).
10. Reis, R. M.; Beati, A. A.; Rocha, R. S. *Ind. Eng. Chem.* **2012**, *51*, 649–654. DOI: <https://doi.org/10.1021/ie201317u>.
11. Paz, E. C.; Aveiro, L. R.; Pinheiro, V. S. *Appl. Catal. B.* **2018**, *232*, 436–445. DOI: <https://doi.org/10.1016/j.apcatb.2018.03.082>.
12. Robles, I.; Moreno-Rubio, G.; García-Espinoza, J. D.; Martínez-Sánchez, C.; Rodríguez, A.; Meas-Vong, Y.; Rodríguez-Valadez, R.; Godínez, L. J. *Environ. Chem. Eng.* **2020**, *8*, 5, 104414. DOI: <https://doi.org/10.1016/j.jece.2020.104414>.
13. Zhang, L. Y.; Wang, M. R.; Lai, Y. Q.; Li, X. Y. *J. Power Sources.* **2017**, *359*, 71–79. DOI: <https://doi.org/10.1016/j.jpowsour.2017.05.056>.
14. Ortiz-Martínez, A. K.; Godínez, L. A.; Martínez-Sánchez, C.; García-Espinoza, J. D.; Robles, I. *Electrochim. Acta.* **2021**, *390*, 138861. DOI: <https://doi.org/10.1016/j.electacta.2021.138861>.
15. Dhelipan, M.; Arunchander, A.; Sahu, A. K.; Kalpana, D. J. *Saudi Chem. Soc.* **2017**, *21*, 487–494. DOI: <https://doi.org/10.1016/j.jscs.2016.12.003>.
16. Chung, D. Y.; Son, Y. J.; Yoo, J. M. *ACS Appl. Mater. Interfaces* **2017**, *9*, 41303–41313. DOI: <https://doi.org/10.1021/acsami.7b13799>.
17. Akula, S.; Sahu, A. K. *J. Electrochem. Soc.* **2019**, *166*, F93–F101. DOI: <https://doi.org/10.1149/2.0441902jes>.
18. Srinu, A.; Peera, S. G.; Parthiban, V. *ChemistrySelect.* **2018**, *3*, 690–702. DOI: <https://doi.org/10.1002/slct.201702042>.
19. Tovar, A. K.; Godínez, L. A.; Espejel, F.; Ramírez-Zamora, R. M.; Robles, I. *Waste Manag.* **2019**, *85*, 202–213. DOI: <https://doi.org/10.1016/j.wasman.2018.12.029>.
20. Giraldo, S.; Robles, I.; Ramirez, A.; Florez, E.; Acelas, N. *SN Appl. Sci.* **2020**, *2*, 1029. DOI: <https://doi.org/10.1007/s42452-020-2736-x>.

21. Oickle, A. M.; Tarasuk, A. C.; Goertzen, S. L. *Carbon*. **2009**, *48*, 1–9. DOI: <https://doi.org/10.1016/j.carbon.2009.11.050>.
22. Fulazzaky, M. A.; *Environ. Nanotechnol.* **2019**, *12*, 1100230. DOI: <https://doi.org/10.1016/j.enmm.2019.100230>.
23. Di, L.; Kerns, E.H. in: *Drug-Like Properties*. Second Ed., Academic Press, **2016**, 307–312. DOI: <https://doi.org/10.1016/C2013-0-18378-X>.
24. Adan-Mas, A.; Alcaraz, L.; Arévalo-Cid, P. *Waste Manag.* **2021**, *120*, 280–289. DOI: <https://doi.org/10.1016/j.wasman.2020.11.043>.
25. Švancara, I.; Schachl, K. *Chem. Listy*. **1999**, *93*, 498–499.
26. O’Sullivan, D. W.; Tyree, M. *Int. J. Chem. Kinet.* **2007**, *39*, 457–461. DOI: <https://doi.org/10.1002/kin.20259>.
27. Nyamful, A.; Nyogbe, E. K.; Mohammed, L. *Ghana J. Sci.* **2021**, *61*, 91–104. DOI: <https://doi.org/10.4314/gjs.v61i2.9>.
28. Vela-Carrillo, A.Z.; Martínez, R. J.; Godínez, L. A.; Pérez-Bueno, J. J.; Espejel Ayala, F.; Robles, I. *Biomass Convers. Biorefin.* **2022**. DOI: <https://doi.org/10.1007/s13399-022-02367-7>.
29. Paul, E.; Vannke, M. A. *Carbon*. **1991**, *31*, 721–730.
30. Chen, N.; Pilla, S. *JCOMC*. **2022**, *7*, 100225. DOI: <https://doi.org/10.1016/j.jcomc.2021.100225>.
31. Gupta, A., Mohanty, A. K.; Misra, M. *JCOMC*. **2022**, *154*, 106759. DOI: <https://doi.org/10.1016/j.compositesa.2021.106759>.
32. Moraes, A.; Assumpção, M. H. M. T.; Simões, F. C. *Electrocatalysis*. **2016**, *7*, 60–69. DOI: <https://doi.org/10.1007/s12678-015-0279-5>.
33. Assumpção, M. H. M. T.; De Souza, R. F. B.; Rascio, D. C. *Carbon*. **2011**, *49*, 2842–2851. DOI: <https://doi.org/10.1016/j.carbon.2011.03.014>.
34. Lu, Z.; Chen, G.; Siahrostami, S. *Nat. Catal.* **2018**, *1*, 156–162. DOI: <https://doi.org/10.1038/s41929-017-0017-x>.
35. Hashemian, S.; Salari, K.; Yazdi, Z. A. *J. Ind. Eng. Chem.* **2014**, *20*, 1892–1900. DOI: <https://doi.org/10.1016/j.jiec.2013.09.009>.
36. Fernandez, M. E.; Nunell, G. V.; Bonelli, P. R.; Cukierman, A. L. *Ind. Crops Prod.* **2014**, *62*, 437–445. DOI: <https://doi.org/10.1016/j.indcrop.2014.09.015>.
37. Cummings, E. A.; Eggins, B. R. *Analyst*. **1998**, *123*, 1975–1980. DOI: <https://doi.org/10.1039/a804021d>.
38. Estrada-Aldrete, J.; Hernández-López, J. M.; García-León, A. M.; Prealta-Hernández, J. M.; Cerino-Cordeva, F. J. *Electroanal. Chem.* **2020**, *857*, 113663. DOI: <https://doi.org/10.1016/j.jelechem.2019.113663>.
39. Bard, A.J.; Faulkner, in: *L.R. Fundamentals and applications*, 2nd Edition, Ed., John Wiley & Sons, Incorporated, United States of America, **2000**, 590–594.
40. Švancara, I.; Hvizdalová, M.; Vytrás, K. *Electroanalysis*. **1996**, *8*, 61–65. DOI: <https://doi.org/10.1002/elan.1140080113>.
41. Švancara, I.; Kalcher, K.; Walcarus, A.; Vytrás, K. *CRC Press*. **2012**. DOI: <https://doi.org/10.1201/b11478>.
42. Chmiola, J.; Yushin, G.; Dash, R.; Gogotsi, Y. *J. Power Sources*. **2006**, *158*, 765–772. DOI: <https://doi.org/10.1016/j.jpowsour.2005.09.008>.
43. Frackowiak, E. *Phys. Chem. Chem. Phys.* **2007**, *9*, 1774–1785. DOI: <https://doi.org/10.1039/b618139m>.
44. Kötz, R., Carlen, M. *Electrochim. Acta*. **2000**, *45*, 2483–2498. DOI: [https://doi.org/10.1016/S0013-4686\(00\)00354-6](https://doi.org/10.1016/S0013-4686(00)00354-6).
45. Rufford, T. E.; Hulicova-Jurcakova, D.; Zhu, Z. J., in: *Green carbon materials advances and applications*, Ed. Pan Stanford Publishing, CRC Press Taylor & Francis Group, **2014**, 93–110.
46. He, Y.; Zhang, Y.; Li, X. *Electrochim. Acta*. **2018**, *282*, 618–625. DOI: <https://doi.org/10.1016/j.electacta.2018.06.103>.